Maintenance of a Mountain Valley Cold Pool: A Numerical Study

BRIAN J. BILLINGS, VANDA GRUBIŠIĆ, AND RANDOLPH D. BORYS

Desert Research Institute, Reno, Nevada

(Manuscript received 16 December 2004, in final form 10 November 2005)

ABSTRACT

A persistent cold-air pool in the Yampa Valley of northwestern Colorado was simulated with the fifth-generation Pennsylvania State University–National Center for Atmospheric Research Mesoscale Model (MM5). The observed cold-air pool, which was identified by temperature measurements along a line of surface stations ascending the eastern side of the valley, remained in place throughout the day of 10 January 2004. The baseline simulation with horizontal resolution of 1 km, which is close to the resolution of operational regional mesoscale model forecasts, neither matched the strength of the observed cold-air pool nor retained the cold pool throughout the day. Varying the PBL parameterization, increasing the vertical resolution, and increasing the model spinup time did not significantly improve the results. However, the inclusion of snow cover, increased horizontal resolution, and an improved treatment of horizontal diffusion did have a sizable effect on the forecast quality. The snow cover in the baseline simulation was essential for preventing the diurnal heating from eroding the cold pool, but was only sufficient to produce a nearly isothermal temperature structure within the valley, largely because of an increased reflection of solar radiation. The increase of horizontal resolution to 333 and 111 m resulted in a stronger cold-air pool and its retention throughout the day. In addition to improving the resolution of flow features in steep terrain, resulting in, for example, less drainage out of the valley, the increase in horizontal resolution led to a better forecast because of a reduced magnitude of horizontal diffusion calculated along the terrain-following model surfaces. Calculating horizontal diffusion along the constant height levels had a beneficial impact on the quality of the simulations, producing effects similar to those achieved by increasing the horizontal resolution, but at a fraction of the computational cost.

1. Introduction

Whiteman et al. (2001) define two types of cold pools. A diurnal cold pool forms during the evening or night and decays following sunrise the next day. A persistent cold pool lasts longer than one diurnal cycle. Therefore, a cold pool that survives the solar heating of the daylight hours is a persistent one. Persistent cold pools can have significant effects on human activities (Smith et al. 1997; Whiteman et al. 1999). Air pollution can accumulate to unacceptably high levels, liquid precipitation falling into the cold pool can produce freezing rain or drizzle, and cold pools can delay the melting of snow and the breakup of ice on rivers. Despite their significant impact, forecasting the buildup and removal of persistent cold pools remains a challenging problem.

Corresponding author address: Brian J. Billings, Division of Atmospheric Sciences, Desert Research Institute, 2215 Raggio Parkway, Reno, NV 89512.
E-mail: billings@dri.edu

The temperature inversion associated with a valley cold pool may not extend to the top of the surrounding ridges. This will result in a band of relatively warmer temperatures known as a thermal belt (Geiger et al. 1995) partway up the sidewalls. Since a thermal belt can be identified in the surface temperatures ascending the valley slopes, cold-air pooling can be identified even if upper-air measurements are unavailable, as is the case for this study.

Much of the attention regarding cold-air pools has focused on their destruction and the breakup of the valley temperature inversion (Whiteman 1990). Whiteman (1982) identified three patterns of inversion breakup in mountain valleys and observed that destruction of the inversion and development of a deep convective boundary layer did not occur in the wintertime in valleys with extensive snow cover, such as the Yampa Valley of northwestern Colorado. A sensitivity study of the actual maintenance of a persistent cold-air pool in the Columbia basin was performed by Zhong et al. (2001). From these numerical simulations, they found

that the strength of the inversion was controlled by temperature changes aloft. The cold pool formed in the presence of downslope warming to the lee of the Cascade Mountains and was destroyed by cold advection aloft. The presence of low-level cloudiness was not necessary for retention of the wintertime cold pool, but was necessary for a springtime cold pool, which was destroyed when skies were clear. Finally, turbulent mixing at the top of the cold-air pool was not significant in cold-pool destruction. Dynamical mechanisms for cold-pool maintenance were also studied by Zängl (2003, 2005b) for deep Alpine valleys. Cold-air drainage was found to be an important dynamical mechanism controlling the persistence of cold-air pools. The imposed pressure gradient due to the geostrophic wind was important in controlling the amount of drainage from the valley. Once again, turbulent mixing was found to be of minor importance for cold-air-pool erosion.

The formation of cold pools has received much less attention. An idealized study of a cold pool in an elevated sinkhole was performed by Zängl (2005a). Apart from undisturbed clear weather, formation of a cold pool required a small heat capacity of the ground and an effective drying mechanism to prevent the formation of fog.

In this study, we investigate the importance of several factors, such as snow cover, length of simulation, vertical and horizontal resolution, and horizontal diffusion, on the accuracy of real-data numerical simulations of a persistent cold pool. The case examined is a persistent cold pool that occurred in the Yampa Valley in the Colorado Rocky Mountains in early January 2004. The simulation results are compared with observations that were obtained in the Yampa Valley during a field research course.

2. Methodology

a. Topography, observing sites, and observational dataset

The upper Yampa Valley (south of Steamboat Springs, Colorado) is a roughly north–south-oriented valley that cuts through the western slope of the Rocky Mountains for a distance of approximately 70 km (Fig. 1). The valley floor has a width of approximately 3.5 km just south of Steamboat Springs, while the ridge to ridge distance is approximately 11 km. The valley floor lies at an average elevation of 2050 m MSL and rises to average elevations of 2400 m MSL on its western side and over 3000 m MSL on its eastern side. At the top of the eastern summit, at an elevation of 3210 m MSL is the Desert Research Institute's (DRI) Storm Peak Laboratory (SPL) (Borys and Wetzel 1997), which serves as the operations center for a field research course offered by the University of Nevada, Reno and the DRI.

The observational network for this study consists of a line of automated surface stations on the eastern slope of the valley. The mesonet stations are maintained by the Steamboat Ski and Resort Corporation and SPL. They report observations every 15 min at all hours of the day. All stations report temperature and relative humidity, but only stations at higher elevations report wind data. Unfortunately, this precludes comparisons of winds above and below the inversion. Additionally, none of the stations reports pressure, so the potential temperatures could not be calculated. Thus, we deal solely with temperatures. The temperature sensors have a range of $-40°$ to $+60°$C and are accurate to $\pm 0.3°$C at 0°C.[1]

Certain stations were eliminated from the dataset because of apparent biases in temperature and humidity. In addition, stations were excluded if their location deviated significantly from the east–west line formed by the majority of the stations. The remaining stations follow a relatively straight path up the valley sidewall. Temperature data from these stations were used to create cross sections of valley temperature. Upper-air measurements would be useful in studying the vertical structure; however, surface-based measurements have been shown to be effective in the study of cold-air pools (Whiteman et al. 2001).

b. Synoptic overview

Data collection at SPL began on 5 January 2004 (the dates in this section correspond to LST), shortly after the passage of a large 500-hPa trough, which had generated a significant amount of snowfall over the area. On 6–7 January, the flow became more zonal, and a pair of minor short waves moved through, creating overcast skies and additional snowfall. On 8 January, flow was from the northwest as a pressure ridge began to build in from the south. This ridge reached a maximum amplitude on 9 January, as its associated upper-level high moved into southwest United States. This high continued north into southwest Colorado on 10 January, but the amplitude of the ridge began to decrease. By the morning of 11 January, the high had dissipated and a cutoff low had moved into the southwest United States.

While the ridge of 8–10 January cleared skies in

[1] More information on these stations is available at Adcon Telemetry Inc., 1001 Yamoto Road, Suite 305, Boca Raton, FL 33431.

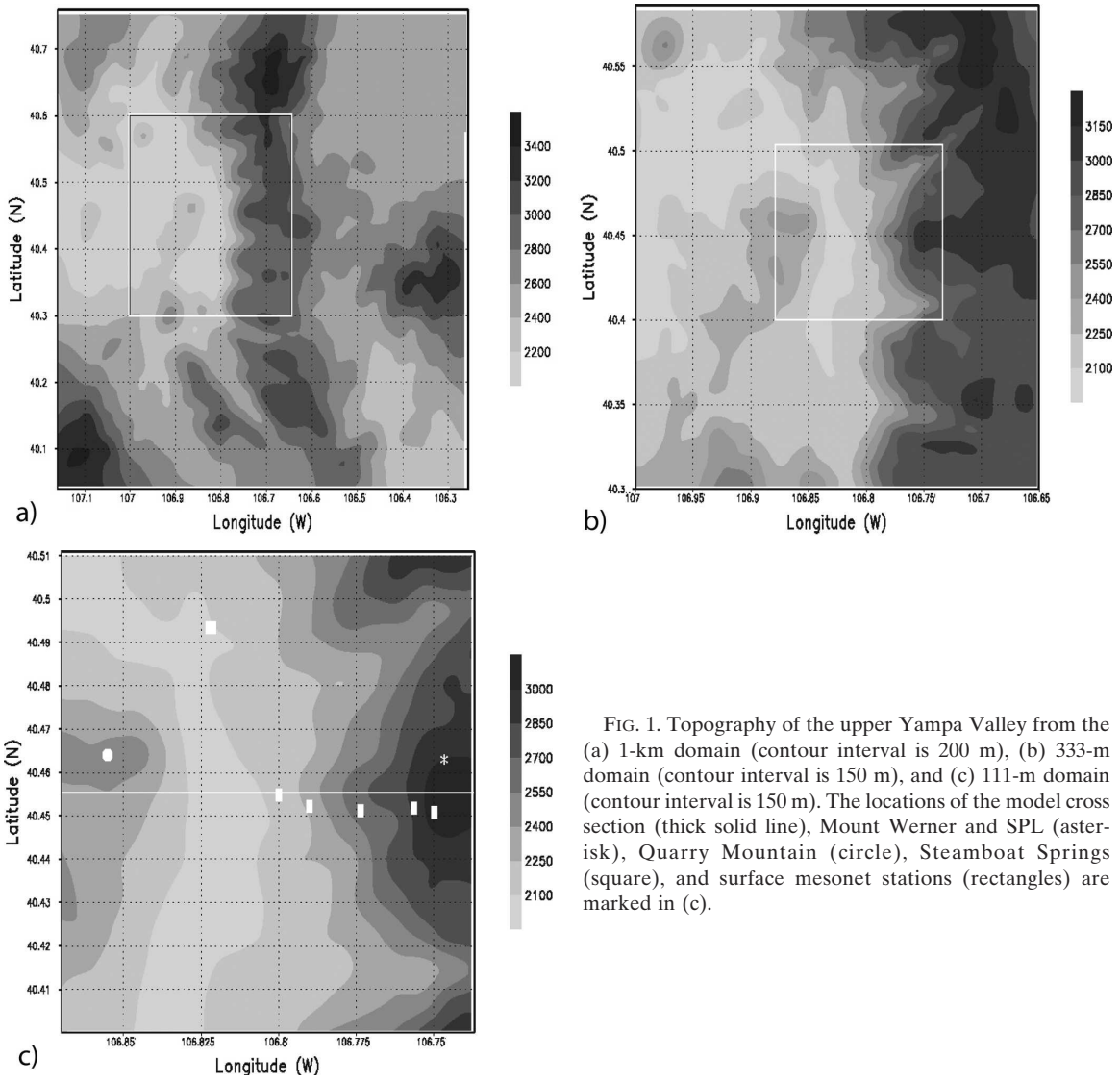

FIG. 1. Topography of the upper Yampa Valley from the (a) 1-km domain (contour interval is 200 m), (b) 333-m domain (contour interval is 150 m), and (c) 111-m domain (contour interval is 150 m). The locations of the model cross section (thick solid line), Mount Werner and SPL (asterisk), Quarry Mountain (circle), Steamboat Springs (square), and surface mesonet stations (rectangles) are marked in (c).

many areas, in certain regions the stagnant flow and recent snowfall led to widespread dense fog, especially in areas influenced by a surface high pressure center, which remained in far eastern Colorado throughout this period. Mount Werner remained enveloped in clouds until clearing occurred during the afternoon and evening of 9 January. At areas farther down the slope, the fog dissipated on the afternoon of 8 January, but in the lowest portion of the valley (i.e., below the height of Quarry Mountain) fog redeveloped during the evenings of 8 and 9 January. This fog dissipated shortly after sunrise on 10 January, and the rest of the day was mostly clear, with the exception of significant contrail activity in the morning that lasted approximately 90 min. An inversion formed in the valley shortly after sunset on 8 January. Despite clearer skies, the cold pool survived each diurnal cycle for four more days, until the field experiment ended, and data were no longer saved. The choice was made to simulate this cold pool for one solar heating period, which was later extended to one diurnal period, that of 10 January 2004.

c. *Numerical model simulations*

The model used in this study was the fifth-generation Pennsylvania State University–National Center for Atmospheric Research Mesoscale Model (MM5; Grell et al. 1994). The baseline simulations contained four nested two-way-interactive domains, all roughly centered over the field site, with resolutions of 27, 9, 3, and 1 km. All of the nests were run for the entire length of

the simulation. In the vertical, 51 sigma levels were used, with finer resolution in the lowest levels of the atmosphere corresponding to approximately 20 m. Terrain elevation, land–water mask, and vegetation data were taken from the U.S. Geological Survey dataset of the corresponding resolutions. Initial and boundary conditions, including snow cover analysis, were provided by the National Centers for Environmental Prediction Global Forecast System (GFS) model reanalyses, with a horizontal resolution roughly equivalent to 55 km. All of the runs used the MM5's Grell cumulus parameterization, Dudhia simple ice microphysical scheme, and cloud-radiation scheme. The baseline run used the Medium-Range Forecast model (MRF) planetary boundary layer (PBL) scheme (Hong and Pan 1996) and included snow cover analysis. The same parameterizations were used in all nested domains. (Because of the stable conditions, the cumulus parameterization probably did not have an effect on the smaller-resolution grids.) The time period for the baseline model simulations was 1200 UTC (0500 LST) 10 January 2004–0000 UTC 11 January (1700 LST 10 January) 2004. The baseline model run was initialized with the GFS reanalysis at the start of this baseline period.

Because the evolution of inversion breakups studied by Whiteman (1982) depended on snow cover and the growth of a convective boundary layer, two factors were initially examined: 1) the use of snow cover analysis and 2) the choice of the PBL parameterization. For the latter, five of the MM5's seven available PBL parameterizations (excluding the simplified bulk and computationally expensive high-resolution Blackadar schemes) were used. In addition to the MRF PBL scheme of the baseline run, we have used the Burk–Thompson PBL scheme (Burk and Thompson 1989), the Eta PBL (Janjić 1994), the Gayno–Seaman PBL (Shafran et al. 2000), and the Pleim–Chang PBL (Pleim and Chang 1992). These parameterizations can be divided into two major groups. The MRF and Pleim–Chang PBL use a simple diffusion scheme with the nonlocal-K approach (Hong and Pan 1996). The other three parameterizations use higher-order turbulence closure based on the Mellor and Yamada (1974) equations.

Based on the results of these simulations, additional sensitivity runs were performed, in which the following parameters were changed: 1) vertical resolution (to better resolve the valley temperature inversion), 2) model start time (to allow additional spinup time for model physics), 3) horizontal resolution (to better resolve the flow within the valley), and 4) horizontal diffusion scheme [to minimize numerical errors discussed by Zängl (2002)].

3. Results

a. The baseline simulation

Figure 2 shows the evolution of the observed temperature profile across the valley from before sunrise to after sunset on 10 January compared with that from the baseline simulation. The observations clearly define a thermal belt located midway up the valley's eastern slope. This feature remains in place throughout the day while temperatures rise significantly, except at the station near the summit. Three hours into the model simulation (Fig. 2a), there is a temperature maximum near the same elevation as seen in the observations and a relative minimum at the valley floor. (By this time, the model has removed a pair of temperature artifacts, sharps spikes of higher temperature on the valley floor, that were in the initial conditions, likely caused by interpolation of the analysis to the high-resolution grid. The effect of these artifacts will be discussed shortly.) The simulated temperatures above the inversion match the observations well, but the temperatures within the cold pool were not as low as observed. It should be noted that the temperature at the lowest mesonet station varied significantly during the early morning hours, with temperatures varying by over 3 K in consecutive 15-min intervals. These changes were well correlated with changes in relative humidity and fog density. However, the station was never as warm as simulated by the model.

After sunrise, the model solution quickly diverges from the observations. Three hours later (Fig. 2b), the temperature in the valley is nearly isothermal at the approximate melting point for ice. During the warmest part of the day (Fig. 2c), there is a slight temperature maximum located on the valley floor. After sunset (Fig. 2d), a new inversion begins to form. The simulated temperatures at this time are closer to the higher temperatures observed; however, this is likely fortuitous because the observed temperatures are descending to where the simulation remained throughout the day. (As observed, the simulation produced fog in the valley until sunrise. After this, the simulated sky cover was clear, also in agreement with observations.)

b. PBL parameterizations

The baseline simulation setup was used with five different PBL parameterization schemes. Similar results were obtained for all of the PBL schemes (not shown).

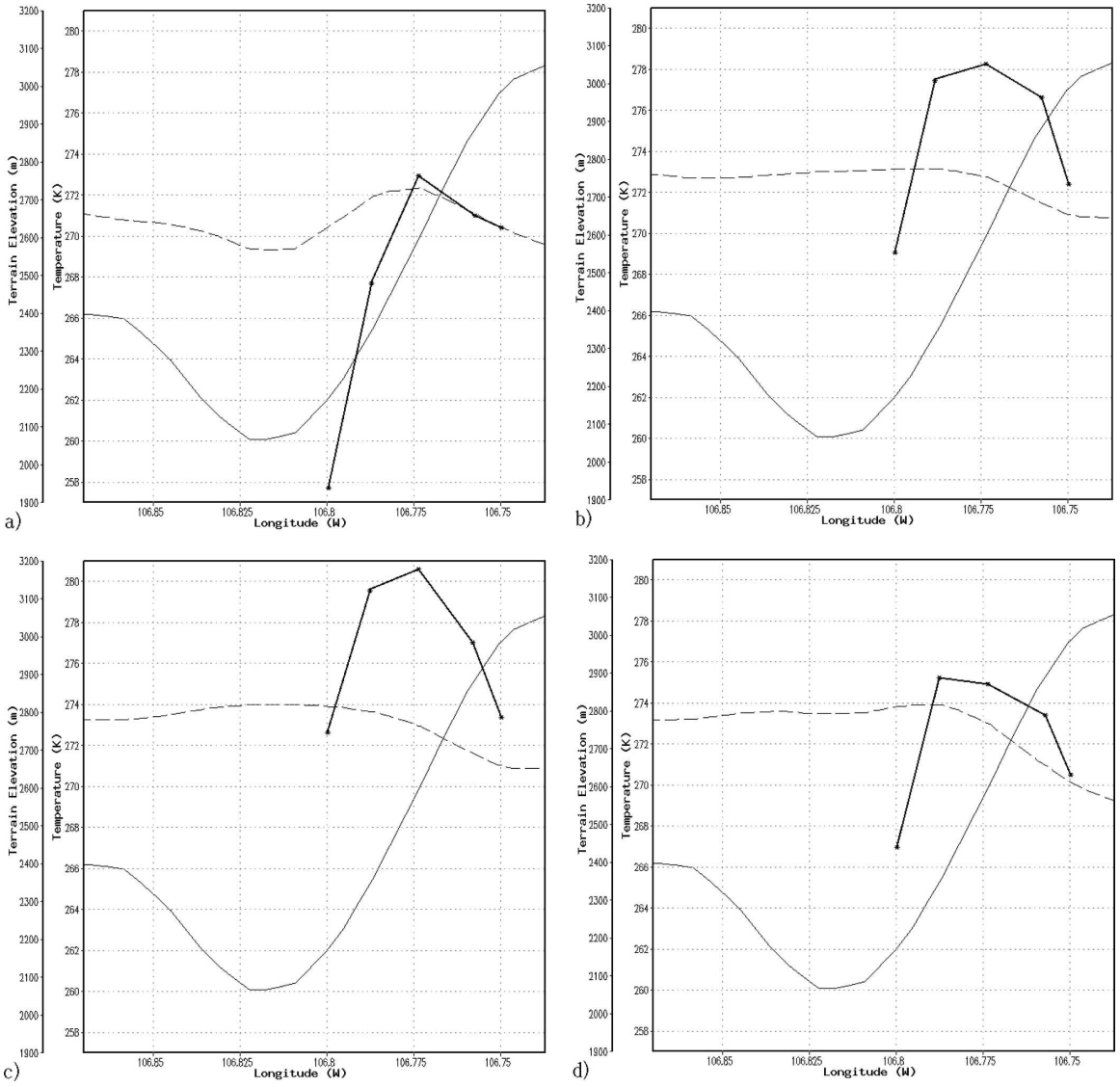

FIG. 2. Cross section of the terrain height (thin solid line), observed temperature (thick solid line), and model-simulated temperature at 1-km resolution along the lowest sigma surface for (a) 1500 (0800 LST), (b) 1800 (1100 LST), and (c) 2100 UTC (1400 LST) 10 Jan 2004, and (d) 0000 UTC 11 Jan (1700 LST 10 Jan) 2004.

The average simulated temperature varied slightly between runs with different schemes, but all of the simulations resulted in nearly identical cross-valley temperature profiles, transitioning from a weak thermal belt during the night and early morning hours through an isothermal pattern to a temperature maximum on the valley floor during the midday.

In the two wintertime inversions observed by Whiteman (1982), growth of the convective boundary layer was arrested at a shallow height. This could explain why these simulations were not sensitive to the choice of the PBL parameterization. Whiteman's (1982) wintertime inversions also occurred in the presence of snow cover, and thus we next explore the importance of this effect for our cold-air-pool simulations.

c. *Snow cover effects*

To determine the importance of snow cover, additional simulations were carried out without snow cover for all five PBL parameterizations. In the absence of snow cover, four of the five PBL parameterizations produced nearly the same result. Figure 3 shows the 24-h temperature profile evolution for the 1-km run with and without snow cover analysis for the MRF scheme. Without snow cover the simulated temperature profiles begin to differ significantly from those

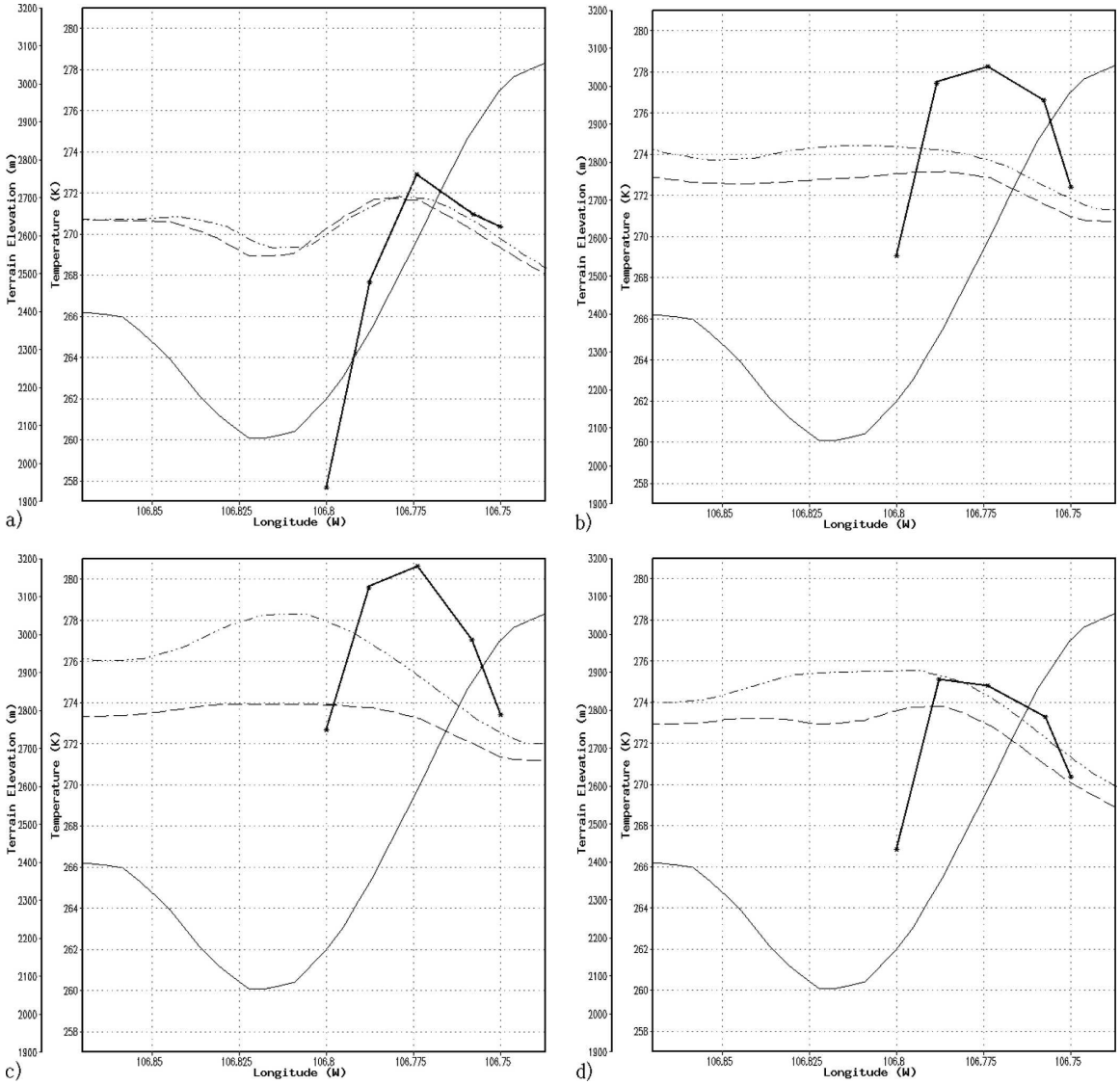

FIG. 3. Cross section of model-simulated temperature at 1-km resolution with snow cover (dashed line) and without snow cover (dot–dashed lines) for the MRF scheme. Terrain, observed temperature, and times are the same as in Fig. 2.

with snow cover once solar radiation commences, leading to an inverse temperature dependence on elevation at midday, with a very distinct maximum at the valley floor and minima on either summit. While neither the simulations with snow cover nor those without it were successful in reproducing the observed temperature profile, the isothermal profiles of the simulations with snow cover were closer to those observed.

Most of the PBL parameterizations are associated with significant differences when snow cover is absent. The exception to this was the Pleim–Chang PBL scheme, which was much less sensitive to snow cover, resulting in similar, though not identical, temperature profiles obtained with and without snow (not shown). This PBL scheme is a combined land surface and PBL model; therefore, it uses a different surface scheme than the other PBL parameterizations in this study (Xiu and Pleim 2001). It appears that because of a simple treatment of snow cover in the Pleim–Xiu land surface model, when the temperatures are below freezing the snow cover has much less effect when temperatures are below freezing (J. E. Pleim 2004, personal communication).

The primary effect of snow cover appears to be an increased albedo. Figure 4 shows time series of outgoing shortwave radiation for the five station locations and the corresponding sensible heat flux. In the presence of snow cover, there is far more reflected solar

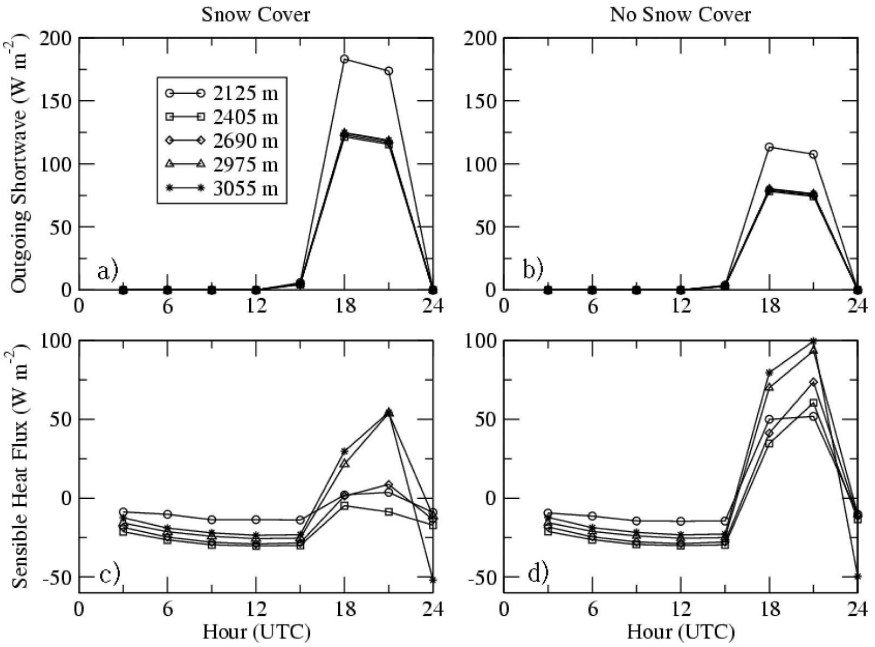

FIG. 4. Simulated time series of outgoing shortwave radiation (a) with and (b) without snow cover. Sensible heat flux is shown in (c) with and (d) without snow cover for the five station locations. These locations are identified by their respective elevations.

radiation, resulting in a lower sensible heat flux, particularly at the lowest three stations, leading to the previously described improvement of the valley temperature profile. The lower temperatures also result in lower values of up- and downwelling longwave radiation. (The lower downwelling values presumably result from less emittance from the surrounding slopes. The larger differences at the lower-elevation station seem to reflect this.) The lower stations also differ from the higher-elevation observations with regard to the effect of snow cover on latent heat flux. The presence of snow cover increases the latent heat flux at the two higher stations (Figs. 5a,b), likely because of increased melting and evaporation. However, for the lowest two stations, the presence of snow cover decreases the latent heat flux. This appears to be related to the changes in relative humidity, which are significantly lower when snow cover is absent. It is possible that this is allowing for increased evaporation and a higher latent heat flux.

When snow cover is present, temperatures in the valley do not rise significantly above the approximate melting point of ice, while the observations exceed +7°C. A constant temperature over melting snow might be expected, so the reasons for the higher station temperatures could be questioned. While the snow cover over the valley was extensive, it is possible that small, isolated areas of snow-free ground were present. Higher temperatures over these areas could then be advected to other regions of the valley. However, this is only speculative, and for the purposes of this study, the mesonet observations will be considered to represent the true temperature values.

d. Additional sensitivity experiments

Because all the simulations that used the baseline model setup were unable to maintain a cold pool in the valley throughout the day, additional simulations were performed in an effort to improve the model forecast. First, the number of vertical levels was increased from 51 to 100 levels, resulting in an approximately 10-m resolution in the lower levels. This did not result in a significant change in the model simulation and the cold-pool maintenance. Then, using the same increased vertical resolution, the model was started 12 h earlier, at 0000 UTC 10 January 2004, so that the model physics had additional time to spin up. As with the higher vertical resolution, the additional spinup time did not significantly change the results of the baseline simulations, particularly during the daylight hours when the isothermal profile dominated the valley. This result does show that the temperature artifacts in the initial conditions did not have a significant impact on the model solutions; however, the longer simulation still did not accurately represent the observations. Nevertheless, the increased vertical resolution and 0000 UTC start time

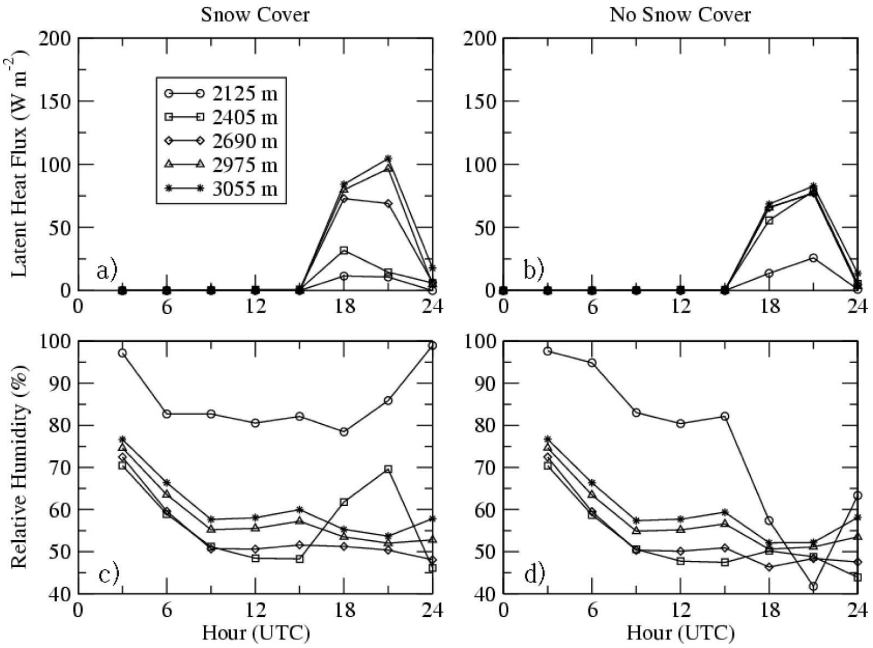

FIG. 5. Same as Fig. 4 but for (a), (b) latent heat flux and (c), (d) relative humidity.

were used in all subsequent model runs to provide additional data for the analysis.

1) HORIZONTAL RESOLUTION EFFECTS

To test the sensitivity to horizontal resolution, we have carried out an additional pair of runs. First, we performed a run with a 333-m domain nested inside the fourth domain of the model setup described at the end of the previous paragraph. Second, a run with 111-m grid spacing in a sixth nested domain was carried out. This was the finest horizontal resolution that could be achieved with a reasonable computation time.

As Fig. 6 shows, with the increased horizontal resolution, the model has retained a weak thermal belt close to the same location as shown by the mesonet observations. The model did seem, however, to still have difficulty increasing the temperature above the freezing point, which may result from the treatment of snow cover by the MM5's land surface models. Despite this, the general features seen in the observations, the cold pool and thermal belt in the valley, have been reproduced to some degree by this simulation. During the first two time periods, before sunrise, there is a very distinct cold pool in the model simulation that matches the observations relatively well with the exception of the minimum temperature in the valley (Fig. 6a). At 1800 UTC (1100 LST), the temperature inversion has started to erode and the magnitude of the cold pool has lessened (Fig. 6b). This is also the time when the midslope mesonet stations begin to warm much faster than in the model simulation. Near the warmest part of the day, the temperature structure still contains a very weak cold pool and thermal belt in the valley (Fig. 6c). At the final time period, after sunset, the cold pool has started to strengthen again, and the model simulations are again in relatively good agreement with the observations (Fig. 6d).

Most of the improvements achieved by increasing the horizontal resolution were direct consequences of better representation of the inversion and resolution of flow features in the valley. For example, the thermal belt covers a horizontal distance of approximately 5 km, and the area of the inversion is half this distance. Therefore, in the 1-km simulation, this feature was covered by only five grid points. The lack of resolution, of course, can be expected to lead to a quick degradation of the forecast. With the horizontal resolution tripled, this same area was covered by 15 grid points, resulting in much improved feature resolution. On the other hand, the observed cold pool was approximately 500 m deep. Thus, the 20-m vertical step was adequate for feature resolution, which explains why doubling the vertical resolution did not significantly improve the forecast. Additional analysis reveals other potential mechanisms for improvement of the simulation because of the finer horizontal resolution.

The vertical cross sections of airflow in the valley

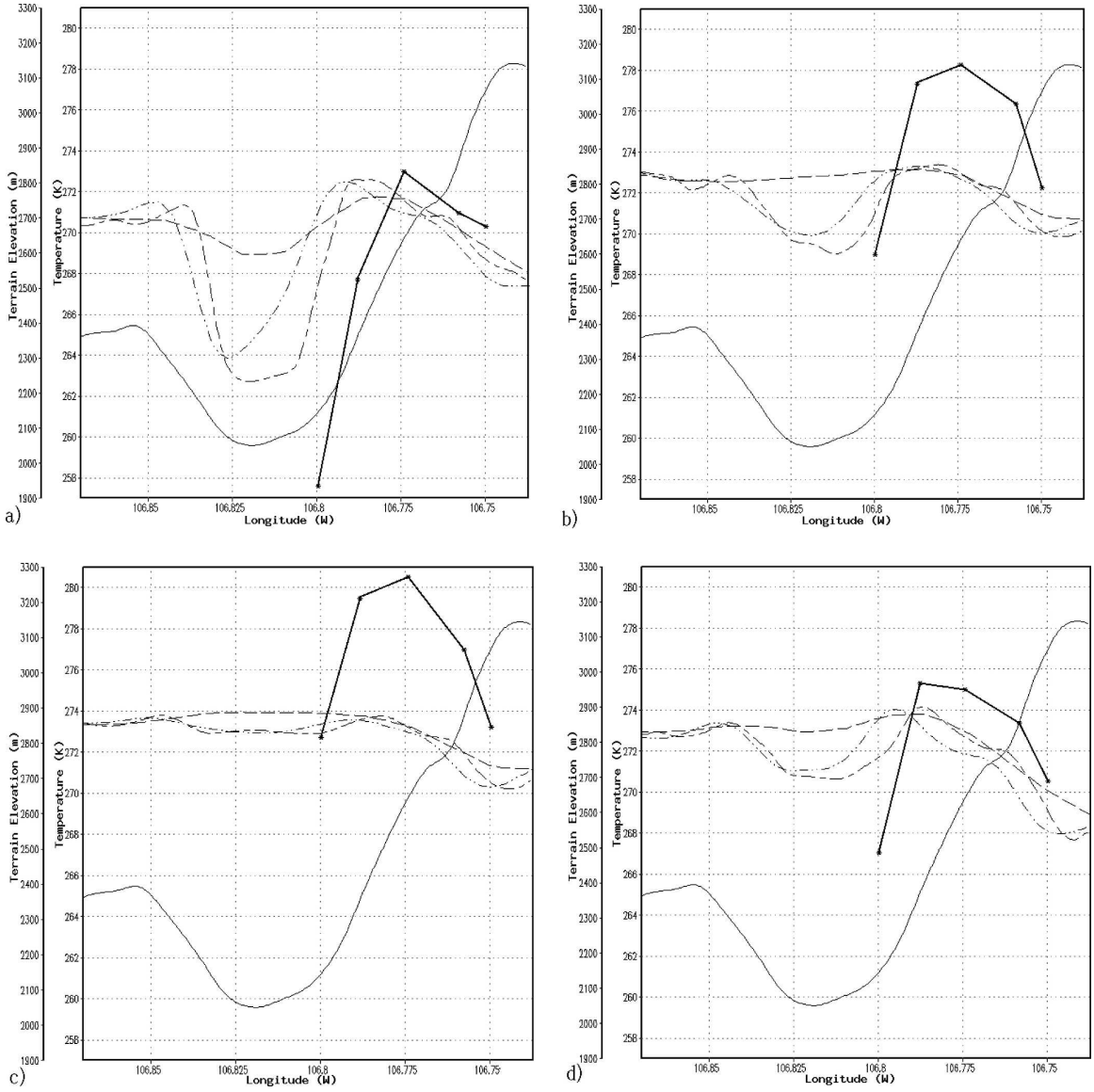

FIG. 6. Cross section of model-simulated temperature for 1-km resolution (dashed line), 333-m resolution (dot–dashed line), and 111-m resolution (short–long dashed line). Terrain, observed temperature, and times are the same as Fig. 2.

were similar at all horizontal resolutions, illustrated by the vertical streamlines from the 333-m simulation in Fig. 7. At approximately the height of the inversion, there is a transition from westerly flow aloft to flow with a weak easterly component within the cold pool. The region where the zonal wind changes from westerly to easterly decreases in elevation during the day, which is consistent with the lowering of the observed inversion. While the inversion is destroyed in the coarser-resolution simulations, an isothermal layer remains, which would be stable enough to prevent penetration of the westerly flow into the valley.

Unlike the airflow in the vertical cross sections, the morphology of the flow in the horizontal changes considerably with increased resolution. Figure 8a shows the horizontal airflow within the cold pool from the 333-m simulation at midday. Flow in the northern half of the Yampa Valley exits the valley toward the northwest. In the southern half of the valley, flow is in an upvalley (toward the south) direction and eventually exits to the south of Quarry Mountain. Over the study area, drainage flows are evacuating air from the valley, with little or no inflow from any source. With the horizontal resolution increased to 111 m (Fig. 8b), a different valley circulation is obtained. Air near the north and south ends of the valley still flows out through passes to the

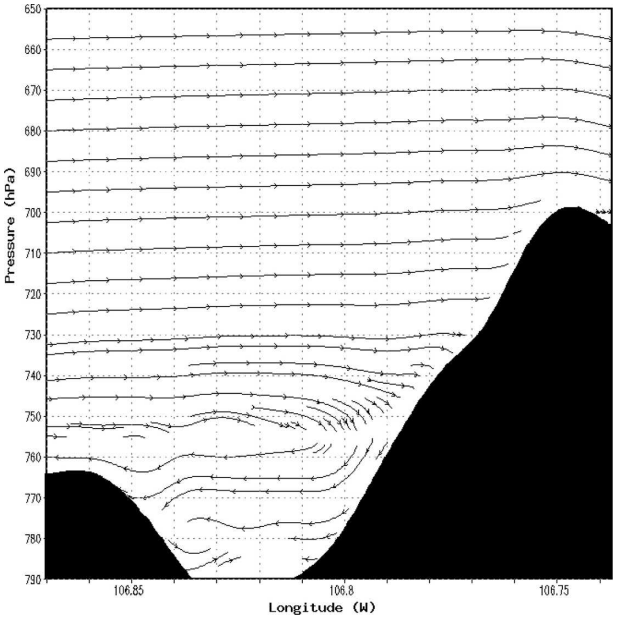

FIG. 7. Flow streamlines in the vertical cross section shown in Fig. 1 at 2100 UTC (1400 LST) from the simulation with 333-m horizontal resolution.

west, but in the center of the valley, there is a downvalley flow along the western slopes and an upvalley flow along the eastern slopes. This leads to a large eddy in the center of the valley that keeps the air circulating in the valley instead of draining out.

While Zängl (2003) showed that drainage flows can play an important role and cause cold pools in open valleys to disappear more quickly than a cold pool in a closed basin, the wind speed in the two runs illustrated in Fig. 8 is on the order of only 1–2 m s^{-1}. Consequently, these different circulation patterns do not significantly affect the results of the simulation. However, in the case of stronger wind speeds, this would be an important mechanism in cold-pool retention.

2) HORIZONTAL DIFFUSION EFFECTS

An additional, indirect effect of increased horizontal resolution is an improved representation of horizontal diffusion. In MM5, horizontal diffusion is calculated with second-order finite differences along the model's terrain-following sigma-coordinate surfaces. At coarse resolution, the adjacent grid points on the same sigma surfaces lie at significantly different elevations. For physical quantities with large vertical gradients (such as temperature), this will lead to significantly different temperatures at neighboring grid points, resulting in large sigma-surface horizontal gradients and overactive horizontal diffusion. In our case, this eventually leads to a uniform temperature profile within the valley. When the horizontal resolution is tripled, the elevation difference between the adjacent grid points along the sigma surfaces is reduced, lessening the effect the vertical temperature gradient has on the horizontal diffusion calculation.

Zängl (2002) demonstrates a less expensive way to correct for these numerical errors, calculating the truly horizontal diffusion by linearly or exponentially interpolating sigma-surface values to a constant height level (see Fig. 1 of Zängl 2002). This horizontal diffusion method has been made available in the MM5, version 3.7, the latest version of the MM5. Consequently, the simulation of the Yampa Valley cold pool was run again using the Zängl (2002) horizontal diffusion scheme.

Figure 9 compares the evolution of the temperature structure in the valley using the Zängl (2002) diffusion scheme with the simulation setup described at the beginning of section 3d. Just prior to sunrise (Fig. 9a), the true horizontal diffusion scheme has produced a more accurate cold pool in the valley. Not only is the temperature difference between the valley floor and midslope greater (in accordance with the observations), but also the maximum of the thermal belt is located farther up the slope, indicating a deeper cold pool, which is again in better agreement with the observations. As solar radiation begins (Fig. 9b), the simulation with the Zängl (2002) diffusion scheme is also not able to match the rapidly increasing observed temperatures, but a far more significant thermal belt is maintained as compared with the previous 1-km simulation. At the warmest part of the day (Fig. 9c), the truly horizontal diffusion scheme has maintained a very weak thermal belt, which did not occur in the previous 1-km simulations. After sunset (Fig. 9d), the simulated cold pool begins to strengthen again, with the maximum of the thermal belt located farther downslope. This descent of the inversion after sunset is also seen in the mesonet observations. While the truly horizontal diffusion scheme yields improvements over the 1-km sigma diffusion simulation, the results are not significantly different from the 111-m simulation with sigma diffusion (cf. Figs. 6 and 9), with the exception of the previously mentioned shift of the thermal belt upslope. This supports the conclusion that increased resolution can lessen the numerical errors of calculating horizontal diffusion along sigma surfaces.

An additional simulation was performed using the Zängl (2002) diffusion scheme at 111-m horizontal resolution. The temperature profiles from this run show more finescale structure of the thermal belt than those from the previous 1-km run, but the results are still

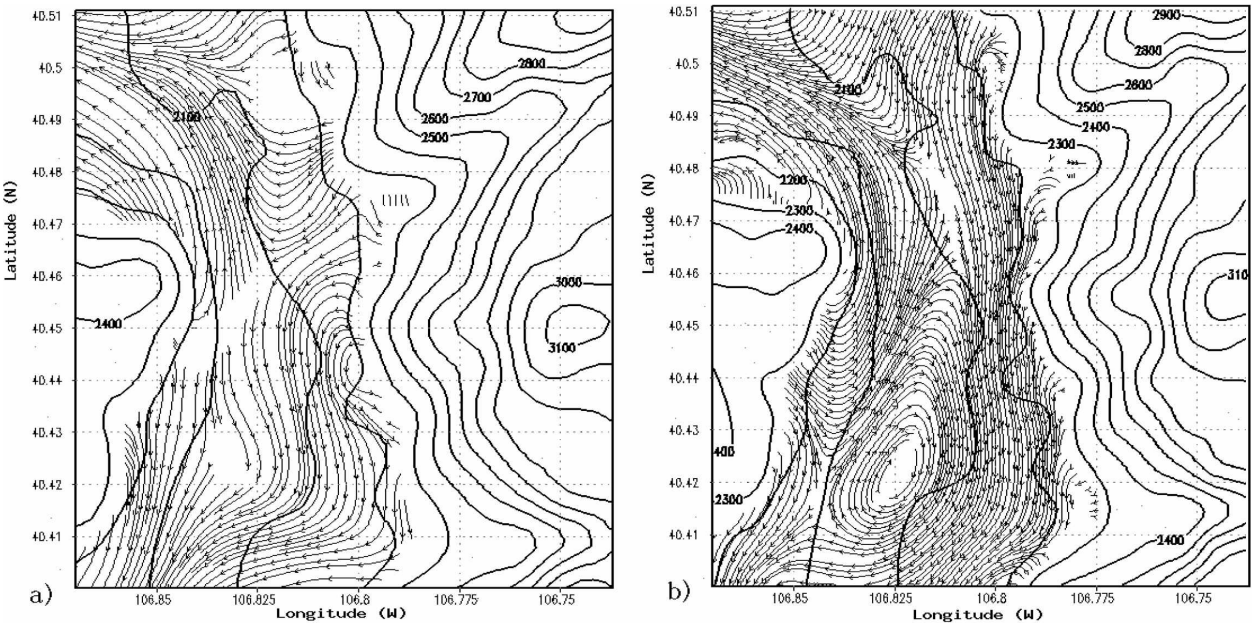

FIG. 8. Horizontal flow streamlines at the 780-hPa level for (a) 333-m resolution and (b) 111-m resolution at 2100 UTC (1400 LST).

generally similar to the 1-km horizontal diffusion and 111-m sigma diffusion simulations over the area of interest. There are larger temperature differences among these runs on the western slope of the valley, but without observations it cannot be determined which of the simulations is the most accurate.

4. Conclusions

A very persistent cold-air pool that remained in the upper Yampa Valley of northwestern Colorado for at least four days was observed in early January 2004. One diurnal cycle of this cold-air pool, on 10 January, was selected for this numerical study. The MM5 model was used for all simulations performed. We have examined the effect of snow cover, choice of PBL parameterization, length of simulation, and horizontal and vertical resolution, as well as formulation of the horizontal diffusion on the forecast of this cold-air-pool's maintenance and strength.

Varying the PBL parameterization, increasing the vertical resolution, and lengthening the simulation did not significantly improve the results. A stronger inversion and maintenance of the cold-air pool throughout the day were obtained by (i) the inclusion of snow cover data in the model, (ii) increasing the horizontal resolution, and (iii) computing the horizontal diffusion on constant height surfaces. Snow cover improved the cold-pool maintenance primarily by increasing the reflected solar radiation. Increased horizontal resolution improved the simulation by improving the resolution of terrain as well as temperature and flow structures within the valley. Computing the horizontal diffusion on constant height surfaces eliminated the excessive diffusion caused by the terrain-following nature of the sigma surfaces and the associated large vertical gradient of temperature. These errors were also reduced by increasing the horizontal resolution, but at a much higher computational cost.

The results of this study emphasize the clear need for accurate snow cover analyses for initialization of operational weather models. In this case, new snow cover was present over an area significantly larger than the valley of interest. However, a greater time after new snowfall, the snow cover may become spatially variable, particularly with respect to elevation, with high-elevation sites retaining snow cover that nearby low-elevation valleys do not. If the model does not capture these variations it will be unable to retain existing cold pools or create artificial cold pools where none are present.

The results also emphasize the importance of horizontal resolution and proper numerical treatment of diffusion in complex terrain simulations. Whereas the 1-km resolution of the unsuccessful baseline simulation is close to that used for operational, regional mesoscale forecasts, the very high horizontal resolutions used in this study, which were a key in reproducing the persistent cold pool, are not likely feasible for operational use in the near future. One solution is to implement a truly horizontal diffusion scheme to eliminate the er-

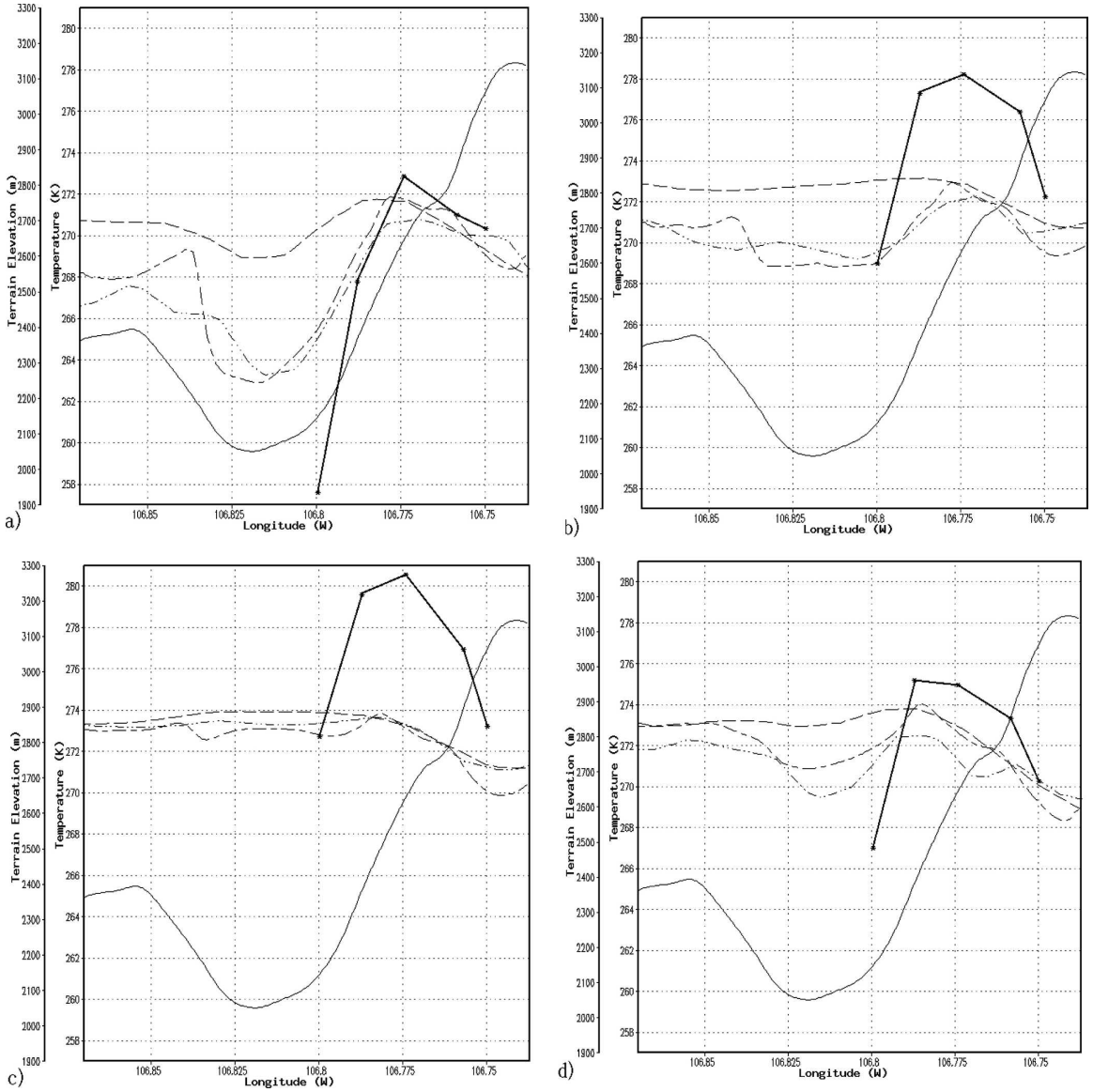

FIG. 9. Cross section of model-simulated temperature at 1-km resolution for sigma-coordinate diffusion scheme (dashed line), Zängl (2002) diffusion scheme (dot–dashed line), and at 111-m resolution for Zängl (2002) diffusion scheme (short–long dashed line). Terrain, observed temperature, and times are the same as in Fig. 2.

rors caused by vertical gradients along sigma surfaces. However, because of all of the consequences of insufficient horizontal resolution discussed here, it remains a responsibility of the local forecaster to understand how larger-scale conditions will be manifest in small valleys that are difficult to resolve.

Although the numerical experimentation significantly improved our model simulation of this cold-air pool from the starting baseline run, the simulated thermal belt is still far weaker than observed. All the simulations with snow cover in this study do not seem capable of significantly exceeding the melting point temperature. More experimentation with the MM5's surface schemes and their representation of snow cover may yield a more accurate result. In addition, other physical parameterizations, besides the PBL schemes, may have an effect on the simulation. Furthermore, the PBL parameterizations used here are not necessarily valid for the simulations with subkilometer horizontal resolution. Schemes more appropriate for these scales are needed in the future.

This study focused on one diurnal period, but the cold pool remained in the valley for a minimum of four days. Studying the entire life cycle of the cold pool

would also be beneficial. The available observations for this case were sufficient only to define the thermal belt and associated cold pool; however, future field programs with more extensive observations, such as tethersondes, dense cross-valley profiles of temperature, or additional surface wind observations, would provide more detailed information on the structure of the cold pools in this valley. Finally, it is important to remember that inversion breakup can vary in different regions and climates (Whiteman et al. 2004). Therefore, caution must be used in extending these results to valleys with different geometries or climate regimes.

Acknowledgments. The first author thanks Drs. Melanie Wetzel and Pat Arnott, who were instructors for the field research course. The logistical support of the Steamboat Ski and Resort Corporation is also acknowledged. The authors also thank Dr. Jonathan Pleim for information on the Pleim–Chang PBL and Dr. David Whiteman for reviewing an early version of this article. The MM5 runs were performed on the Nevada Environmental Computing Grid of the ACES program with assistance from Dr. Shulan Liu and on the Sierra Cluster of the DRI's Mesoscale Dynamics and Modeling Laboratory (MDML) with assistance from Dr. Boro Grubišić. The ACES program (http://www.aces.dri.edu) has been funded by an NSF EPSCoR grant to the Nevada System of Higher Education, and the MDML Sierra Cluster was funded by NSF Grant ATM-0116666 to DRI. This research was supported in part by the NSF Grant ATM-0242886. Figures were drawn with GrADS, created by Brian Doty. DRI is an equal opportunity service provider and employer and is a permittee of the Medicine-Bow and Routt National Forests.

REFERENCES

Borys, R. D., and M. A. Wetzel, 1997: Storm Peak Laboratory: A research, teaching, and service facility for the atmospheric sciences. *Bull. Amer. Meteor. Soc.,* **78,** 2115–2123.

Burk, S. D., and W. T. Thompson, 1989: A vertically nested regional numerical weather prediction model with second-order closure physics. *Mon. Wea. Rev.,* **117,** 2305–2324.

Geiger, R., R. H. Aron, and P. Todhunter, 1995: *The Climate near the Ground.* 5th ed. Vieweg, 528 pp.

Grell, F. A., J. Dudhia, and D. R. Stauffer, 1994: A description of the fifth-generation Penn State/NCAR Mesoscale Model (MM5). NCAR Tech. Note NCAR/TN-398 + STR, 122 pp. [Available from NCAR, P.O. Box 3000, Boulder, CO 80307.]

Hong, S.-Y., and H.-L. Pan, 1996: Nonlocal boundary layer vertical diffusion in a medium-range forecast model. *Mon. Wea. Rev.,* **124,** 2322–2339.

Janjić, Z. I., 1994: The step-mountain eta coordinate model: Further developments of the convection, viscous sublayer, and turbulence closure schemes. *Mon. Wea. Rev.,* **122,** 927–945.

Mellor, G. L., and T. Yamada, 1974: A hierarchy of turbulence closure models for planetary boundary layers. *J. Atmos. Sci.,* **31,** 1791–1806.

Pleim, J. E., and J. S. Chang, 1992: A non-local closure model for vertical mixing in the convective boundary layer. *Atmos. Environ.,* **26A,** 965–981.

Shafran, P. C., N. L. Seaman, and G. A. Gayno, 2000: Evaluation of numerical predictions of boundary layer structure during the Lake Michigan Ozone Study. *J. Appl. Meteor.,* **39,** 412–426.

Smith, R. B., and Coauthors, 1997: Local and remote effects of mountains on weather: Research needs and opportunities. *Bull. Amer. Meteor. Soc.,* **78,** 877–892.

Whiteman, C. D., 1982: Breakup of temperature inversions in deep mountain valleys. Part I: Observations. *J. Appl. Meteor.,* **21,** 270–289.

——, 1990: Observations of thermally developed wind systems in mountainous terrain. *Atmospheric Processes over Complex Terrain, Meteor. Monogr.,* No. 45, Amer. Meteor. Soc., 5–42.

——, X. Bian, and S. Zhong, 1999: Wintertime evolution of the temperature inversion in the Colorado Plateau Basin. *J. Appl. Meteor.,* **38,** 1103–1117.

——, S. Zhong, W. J. Shaw, J. M. Hubbe, X. Bian, and J. Mittelstadt, 2001: Cold pools in the Columbia Basin. *Wea. Forecasting,* **16,** 432–447.

——, B. Pospichal, S. Eisenbach, P. Weihs, C. B. Clements, R. Steinacker, E. Mursch-Radlgruber, and M. Dorninger, 2004: Inversion breakup in small Rocky Mountain and Alpine basins. *J. Appl. Meteor.,* **43,** 1069–1082.

Xiu, A., and J. E. Pleim, 2001: Development of a land surface model. Part I: Application in a mesoscale meteorological model. *J. Appl. Meteor.,* **40,** 192–209.

Zängl, G., 2002: An improved method for computing horizontal diffusion in a sigma-coordinate model and its application to simulations over mountainous topography. *Mon. Wea. Rev.,* **130,** 1423–1432.

——, 2003: The impact of upstream blocking, drainage flow, and the geostrophic pressure gradient on the persistence of cold-air pools. *Quart. J. Roy. Meteor. Soc.,* **129,** 117–137.

——, 2005a: Formation of extreme cold-air pools in elevated sinkholes: An idealized numerical process study. *Mon. Wea. Rev.,* **133,** 925–941.

——, 2005b: Dynamical aspects of wintertime cold-air pools in an Alpine valley system. *Mon. Wea. Rev.,* **133,** 2721–2740.

Zhong, S., C. D. Whiteman, X. Bian, W. J. Shaw, and J. M. Hubbe, 2001: Meteorological processes affecting the evolution of a wintertime cold air pool in the Columbia Basin. *Mon. Wea. Rev.,* **129,** 2600–2613.